ACADEMIC PRESS

Available online at www.sciencedirect.com

SCIENCE DIRECT®

Journal of Sound and Vibration 264 (2003) 157–176

JOURNAL OF SOUND AND VIBRATION

www.elsevier.com/locate/jsvi

Circulation pumps as structure-borne sound sources: emission to semi-infinite pipe systems

N. Qi, B.M. Gibbs*

Acoustics Research Unit, School of Architecture and Building Engineering, University of Liverpool, P.O. Box 147, Liverpool L69 3BX, UK

Received 28 August 2001; accepted 30 May 2002

Abstract

Circulation pumps are an important source of noise from domestic central heating systems. Pumps can generate airborne, liquid-borne and structure-borne sound and although standards exist for airborne and liquid-borne sources, none do for structure-borne sources. This is primarily because the structure-borne acoustic power delivered by the pump not only depends on the pump but also on the connected receiving system, which can be a complicated combination of pipes, valves and radiators. Also pumps deliver liquid-borne and structure-borne acoustic power simultaneously and their relative contributions to the sound radiated from the pipe system is not obviously obtainable. The approach proposed is to estimate the emission from the pump into semi-infinite pipes of material and cross-section typical of heating systems. Then to estimate the 'mixing' effect of bends, joints and other pipe discontinuities, due to wave mode conversion, as described in a companion paper. In the present paper, it is demonstrated that the structure-borne power can be calculated from the measured free velocity and mobility of the pump for each component of vibration and from receiver mobilities of idealized pipe systems. The structure-borne power is compared with the liquid-borne power measured directly by intensimetry.

1. Introduction

Circulation pumps and control valves are the main noise sources in modern hot-water heating systems. The number of circulation pumps in the UK alone runs into tens of millions and they are used in industrial processes, transportation and in homes. Pumps often are the cause of complaints of excessive noise in domestic central heating systems. The problems are seldom the result of direct radiation of sound from the pump housing but rather from liquid-borne sound

*Corresponding author. Tel./fax: +44-151-794-4937.
E-mail address: bmg@liverpool.ac.uk (B.M. Gibbs).

0022-460X/03/$ - see front matter
doi:10.1016/S0022-460X(02)01172-0

transmission through to the pipe system and structure-borne sound transmission which directly excites the pipe walls, radiators, etc., and supporting walls and floors. The installation, as well as the pump, determines the noise.

Therefore, it might be appropriate to measure the radiated sound from a pipe–radiator system typical of domestic installations and rate the pump accordingly. In a preliminary investigation, a pipe–radiator system was assembled in the receiver room of a small transmission suite. Each of a production batch of circulation pumps was installed in the source room and connected to the pipe–radiator system. The pumps were rated according to the spatial average sound level generated in the receiver room. However, the rank order of pumps changed if the pipe–radiator system was altered [1,2]. This might be expected, since if the receiver system is altered, the structural dynamics of the contact point is changed and thence the acoustic power delivered. A further disadvantage of this approach is that it is not possible to establish a hierarchy of power emitted from the pump i.e. is the pump primarily an airborne, structure-borne or fluid-borne source? Each component initially must be treated separately.

For the case of airborne sound sources, characterization by sound power is straightforward and methods are well established [3]. The source impedance is relatively large and the 'constant velocity' source is unaffected by the surrounding air in most situations. This is not always the case and the constant power assumption is tenuous for sources in tightly enclosed spaces [4]. There also has been a large body of work on liquid-borne noise, leading to standards [5–7].

There has been little work on structure-borne sources. In particular, a characterization equivalent to airborne sound power does not exist. There are several reasons for this. For structure-borne sources, the source mobility may not appreciably differ from that of the receiver and possibly may match it [8]. Mobilities are complex functions of frequency and depend on the position of the contact points on source and receiver. In pipes, the structure-borne sound is carried by a combination of bending, axial and torsional waves and there is fluid–structure interaction [9].

The requirement for detailed knowledge of the receiving system can be partially circumvented by considering idealized infinite or semi-infinite receiving structures [10]. This is analogous to anechoic measures of airborne power and allows consideration of essential features of the transmission. The source–path–receiver approach, common for airborne sound problems, becomes a source–transmission–path–receiver approach [11]. Elsewhere, the transmission has been considered in terms of an independent source descriptor [12,13] or the characteristic power [14]. Both employ a matched mobility condition to estimate an upper limit to the power possible from the source. The actual power, when connected to a specific receiving structure, then is some lesser value, obtained by means of a coupling function, which is a function of the mobilities of the source and receiver.

In a preliminary experimental study of pumps connected to pipe systems it was observed that structural discontinuities: bends, supports and connections, plus imperfections in workmanship, cause wave mode conversion, thereby mixing the input powers from the (up to six possible) components of excitation. This leads to the speculation that if the power can be calculated from each component of excitation, into an idealized semi-infinite receiving system, then a hierarchy of contributions can be established which corresponds to that in real pipe system. In this context, the transmission is the power into an idealized receiving system of infinite or semi-infinite extent. The path then is treated as a fluctuation about the trend value obtained, due to reflections and

attenuations at structural discontinuities. A similar approach has been used in estimating power from vibrating machines into floors, where the floor is assumed to be of infinite area [15,16].

In this study, the structure-borne emission is obtained indirectly from measured free velocity and mobility of the pump and from predicted mobility of a semi-infinite pipe of material and cross-section typical of domestic pipes. For comparison, the fluid-borne emission is measured directly by acoustic intensimetry.

2. Airborne sound emission from pumps

It is straightforward to confirm that modern domestic heating pumps are not significant airborne sources. Each of six pumps from a production batch (240 V, 50 Hz, single phase, input watts: 80–112, flow rate: 10–50 l/min for head 5–1.5 m) was placed in a small reverberant room and connected in-line to a pipe–radiator system, located in an adjacent reverberant room. The spatial average sound pressure level was obtained in the room containing the pump under normal operating conditions. In all cases, the spectrum was the same as the background.

3. Structure-borne sound emission

Central heating pumps usually are installed in-line with the piping. The piping, therefore, is the primary transmission path to the far field. The path further divides into that through the enclosed liquid and along the pipe wall.

The internal dynamic forces in a pump that generate vibrations can be termed the activity. The vibrational velocity of the housing or at the contacts with the pipe-work is a map of the activity. If the vibrating pump is unconstrained but otherwise operating under normal conditions, then the free source velocity measured is an independent characteristic of the source if linear conditions are assumed [17–19].

For the velocity measurements, the pumps were connected to pipes to form a circuit for liquid flow. Rigid pipes affect the dynamical loading of the pump and thus the contact velocity. In order to approximate the free source condition, flexible pipes were used to carry the pumped water. This was confirmed by first measuring the velocities at the outlet of the unconnected pump while running 'dry'. The measurements were repeated when connected to the flexible pipes, again without water in the system. The difference in velocity level was about 2 dB below 100 Hz, and 1 dB between 100 and 1200 Hz.

With the pump operating normally (the flow rate typically was 1.2 m/s), three accelerometer-pairs were located on the outlet to record the three translational and three rotational components of velocity. A typical set of results is shown in Fig. 1. The translational velocities have similar values, with an overall slope of about -6 dB/oct. The three angular velocities have more fluctuations, also with an average slope of -6 dB/oct. The rotational velocities are dimensionally incompatible with the translational velocities. It is not possible to assess the importance of a component of vibration, in terms of the structure-borne power delivered in an installed condition, from inspection of these curves alone. Therefore, although the free velocity is a map of the pump

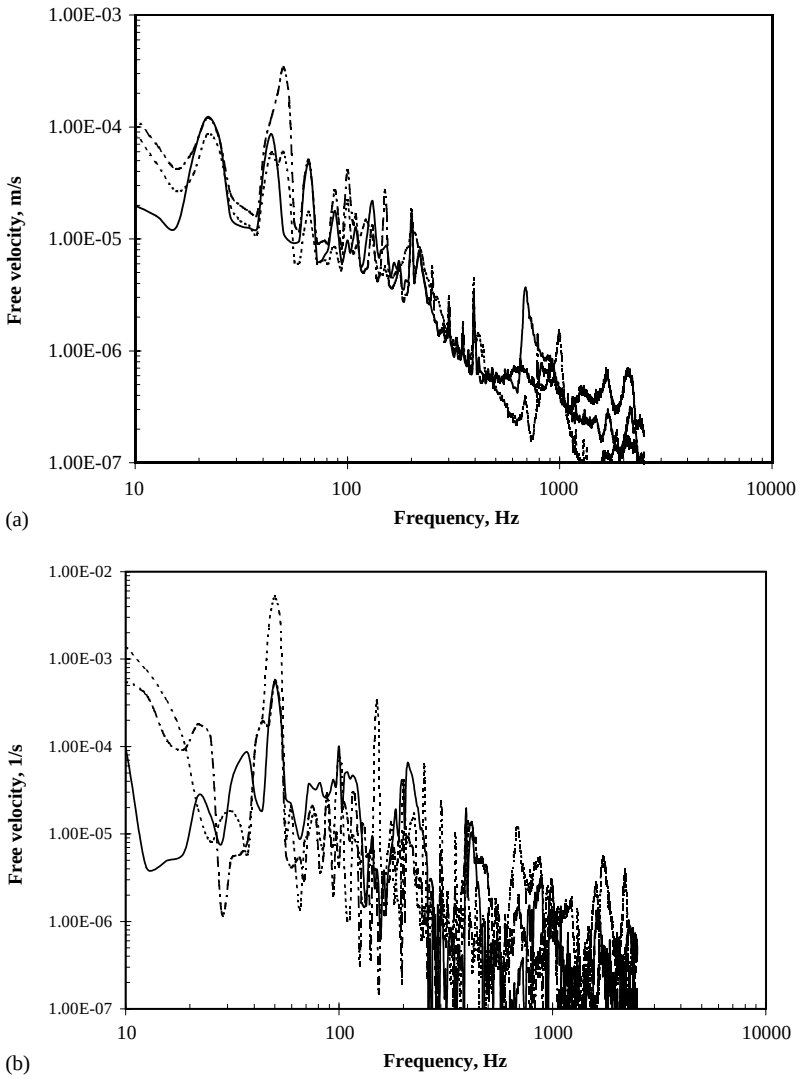

Fig. 1. (a) Three translational components of free velocity: ——, v_x; –·–·–, v_y; - - - - - -, v_z. (b) Three angular components of free velocity: ——, w_x; –·–·–, w_y; - - - - - -, w_z.

activity, it is not a full structure-borne characterization. Pumps of the same free velocity may yield different sound levels when installed, because the pumps may have different source mobilities.

Consider the active power from a pump of free velocity v_{sf} and source mobility $\tilde{Y}_s$, connected to a pipe system of receiver mobility $\tilde{Y}_r$:

$$P = \frac{1}{2}\frac{(v_{sf})^2}{\left|\tilde{Y}_s + \tilde{Y}_r\right|^2}\,\mathrm{Re}\{\tilde{Y}_r\}. \tag{1}$$

Three quantities are required, for each component of excitation and for each contact. The mobility is the complex ratio of the translational or rotational response velocity taken at a point in

a system, to the exciting force or moment phasor at the same point or another point in the system [20]. Mobility is frequency dependent and is a function of structure geometry, boundary conditions and material properties. The terms point, transfer and cross mobility designate a location and direction with respect to the two vectors. In this study, the point force mobility was most frequently used, where

$$\tilde{Y} = \frac{v}{F}. \tag{2}$$

The force and response are on the same point and in the same direction. The translational mobility was obtained using standard techniques [21] and one of the results is shown in Fig. 2 from a batch of nine compact pumps, made of iron with a mass of 2 kg. Also shown is the predicted mobility for a rigid body of the same mass as the pump. A rigid bodied characteristic is indicated, up to the anti-resonance at a frequency of 2 kHz. In this frequency range, point mobility measurements are appropriate. Above this frequency the response is stiffness and resonance controlled.

The corresponding moment mobility is given by

$$\tilde{Y}_\omega = \frac{w}{M}, \tag{3}$$

where M is the applied moment and w is the rotational response velocity. The co-ordinate system is shown in Fig. 3. The moment mobilities were obtained by using a direct method according to Petersson [22,23] where moment was imparted by means of a seismic mass and two giant magnetostrictive rods, operating out of phase. The moment imparted is proportional to the rotational acceleration of the seismic mass, recorded by means of an accelerometer pair. A second accelerometer pair, attached to the pump, gives the rotational velocity. In Fig. 4 are shown results for the three moment mobility components.

A full mobility matrix description of power is usually intractable and does not give a transparent insight into the important transmission components [24,25]. An alternative is to establish a hierarchy of input powers from consideration of the main components of structure-borne propagation along semi-infinite pipes. The approach requires measurement or prediction of

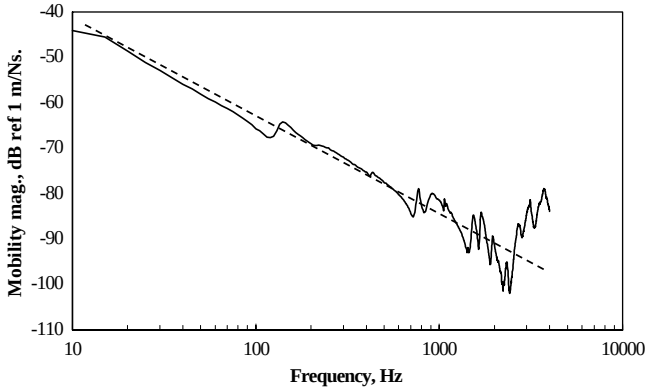

Fig. 2. Point force mobility magnitude: ——, measured; - - - - - - -, predicted.

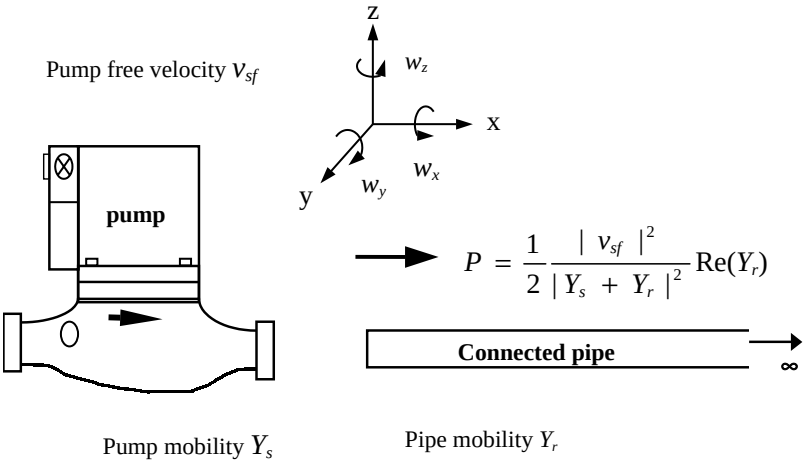

Fig. 3. The active power transmitted from pump to connected pipe. Also shown is the co-ordinate system.

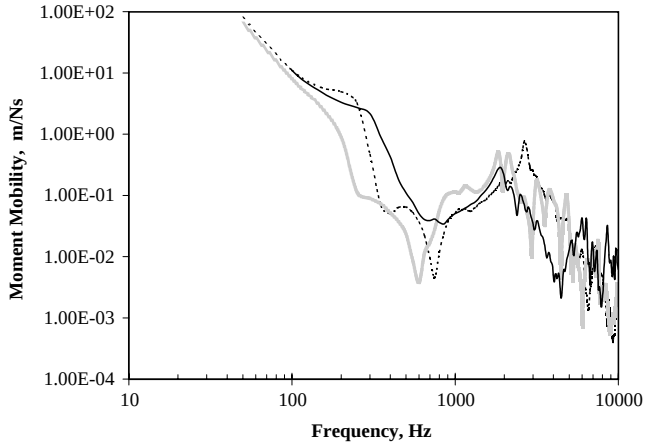

Fig. 4. Magnitude of moment mobility: ——, $\tilde{Y}_{\omega x}$; ——, $\tilde{Y}_{\omega y}$; - - - - - -, $\tilde{Y}_{\omega z}$.

the pump mobilities, measurement of the pump free velocities and prediction of the infinite pipe mobilities.

4. Source descriptor

Prior to considering power into semi-infinite pipes according to Eq. (1), the source descriptor concept [12] was invoked in order to establish a preliminary hierarchy of excitation components. The complex power, given in Eq. (6), is expressed as a product of the source descriptor $\tilde{S}$ which describes the ability of a source to deliver power, and the coupling function $\tilde{C}_f$ which relates to the dynamic properties of the contact point between the two structures. The two

functions are given as

$$\tilde{S} = \frac{1}{2}\frac{\left|V_{sf}\right|^2}{\tilde{Y}_s^*}, \tag{4}$$

$$\tilde{C}_f = \frac{\tilde{Y}_s^* \tilde{Y}_r}{\left|\tilde{Y}_s + \tilde{Y}_r\right|^2}. \tag{5}$$

The complex power then is

$$\tilde{P} = \tilde{S}\tilde{C}_f \tag{6}$$

The active power is given by the real part of $\tilde{P}$ in Eq. (6). The source descriptor is an independent source property. It requires only source variables, which are practically measurable for most pumps. It has the units of power; different components of motion can be compared directly and can be summed to form a single value.

In Fig. 5 are shown the six source descriptor components for the pump type investigated, for the frequency range 10 Hz to 2.5 kHz. The advantage of the source descriptor approach is highlighted. A hierarchy of component powers is obtained without needing to consider a receiving structure. Over most of the frequency range of interest, the rotational components are 20 dB lower than the translational components. It therefore was assumed that the rotation components of pump excitation could be neglected. This assumption is allowed because the treated receiving structure is semi-infinite. However, in real pipe systems, the pump may be connected to a short pipe and moment mobility and cross-mobility terms may assume importance [26]. The rotational components then may become important and, therefore, the assumption must be treated with some caution.

The important excitation components are influenced by the important propagation modes in pipe systems, now described.

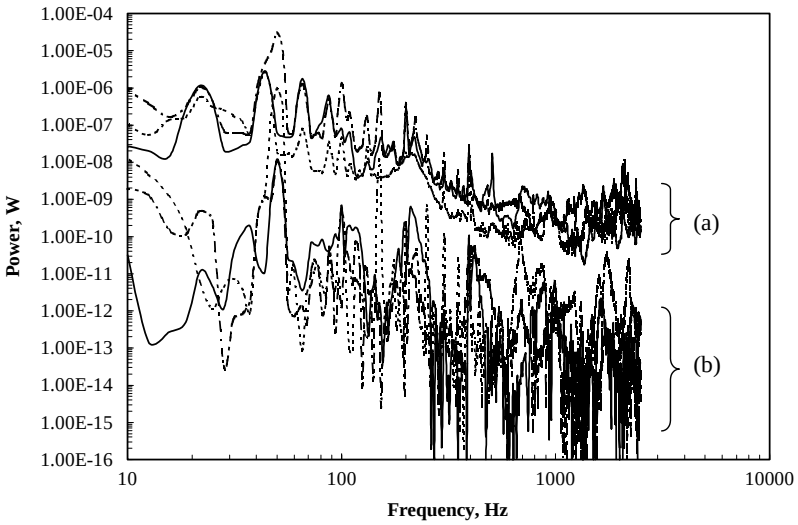

Fig. 5. Six components of the source descriptor for the pump: (a) translational components, (b) rotational components.

5. Vibration wave types in liquid-filled pipes

The theory of waves in fluid-filled cylindrical elastic shells is contained in Refs. [27–29]. The derivation of the equations of vibration of circular cylindrical shells can be found in Refs. [30–32]. The free, simple harmonic motion of a thin-walled cylindrical shell containing an acoustic field can be described by the Donnell–Mushtari shell equations [33]. A mode, in this context, is defined as an allowed displacement variation with respect to circumference, which can exist at a certain frequency in an infinitely long shell. It is independent of all other modes. To find the modes that can exist on a pipe, the equations are derived and the solutions depend on the approximations that are used for deriving the equations of motions. Leissa [32] summarizes the results of the so-called zero-order approximations, which neglect shear deformation and rotational inertia in the pipe wall. An in vacuo vibrating shell exhibits three real axially symmetric modes (out of four possible), while for liquid-filled shells this number is unlimited [28].

Expressions are given in terms of a non-dimensional frequency $\Omega = f/f_{ring}$, where the ring frequency $f_{ring} = 1/2\pi R\sqrt{E/\rho_p(1-\mu^2)}$. There are three axially symmetric modes that start at zero frequency. They have real wave numbers at all frequencies and are measurable, as demonstrated by Pinnington and Briscoe [33] who used external sensors to register the waves in liquid-filled pipes. The first ($n = 0$) corresponds to a torsional wave in a circular cylindrical rod. The circumferential motion is uncoupled with the axial and radial motions. Also, because the viscosity effects are small, the vibrations in the pipe wall are uncoupled with the contained liquid so that this mode is equal to that in vacuo. The velocity of a torsional wave is independent of frequency and is weakly dependant on the cross-section.

The second mode is close to the in vacuo quasi-longitudinal shell mode. There is no circumferential motion but the axial motion is coupled with the radial motion by the Poisson effect, and thus to the contained liquid. At frequencies well below the ring frequency, the mode corresponds to a quasi-longitudinal wave in a thin plate [34]. The third mode approximates a plane duct wave. However, because of flexibility of the pipe wall, the phase velocity is dependent on wall thickness and frequency.

Consider a water-filled copper pipe with $R = 11$ (mm), $E = 12.2 \times 10^{10}$ (Pa), $\rho_p = 8900$ (kg/m^3) and for $\Omega \ll 1$. From White and Sawley [35], the phase velocity $c_f' \cong 0.45c_f$, where c_f is the plane wave velocity in a rigid wall pipe (about 1500 m/s in water). The pipe wall flexibility lowers the velocity to less than half of that in the rigid pipe, but for copper pipe, commonly used in central heating systems, the cut-off frequencies of higher order duct modes still remain far above the frequency range of interest.

There is one first order mode ($n = 1$) that starts at zero frequency. At frequencies far below the ring frequency, this mode corresponds to a bending wave in a slender beam. Leissa [32] and Fuller [34] show that the equivalence of the first order mode to a bending wave on a slender beam is valid in the frequency range in which rotational inertia and shear can be neglected [31].

The bending wave velocity is reduced due to the mass loading effect of the liquid. For $h/R \ll 1$ the mass per unit length may be approximated by

$$m' = 2\pi Rh\rho_p + \pi R^2\rho_f. \tag{7}$$

For a water-filled copper pipe with $R = 0.011$ m and $h = 0.0009$ m, m' is increased by a factor of 1.7 compared with the in vacuo case. According to Eq. (7), this results in a reduction of the wavelength by a factor $\sqrt[4]{1.7} \cong 1.14$.

Zero order theories predict two second order modes that commence at non-zero frequencies. Expressions for the cut-off frequency are summarized and presented by Leissa [32]. The lower cut-off frequency for $n = 2$ on the copper pipe with $R = 0.011$ m and $h = 0.0009$ m is 3630 Hz. A formula for the lower $n = 2$ cut-off frequency of liquid filled pipes can be obtained from Ref. [36]. For the water-filled copper pipes with dimensions as above, the lower $n = 2$ cut-off frequency is 2915 Hz. These frequencies are above the frequency range 20–2500 Hz of interest, so that modes for $n = 0$ and 1 were considered only.

6. Energy distributions in liquid-filled pipes

From the previous discussion it can be seen that at low non-dimensional frequencies, four propagating waves occur in fluid-filled pipes: torsional, quasi-longitudinal and two bending waves. Each of these waves carries energy in the pipe wall, while quasi-longitudinal and bending waves also carry energy in the liquid. The degree to which the energy is concentrated in the liquid or the pipe wall depends upon the type of excitation of the pipe and the physical parameters of the pipe wall and the contained liquid [33]. Fuller and Fahy [27] have found that at low frequencies ($\Omega < 1$) for the $n = 0$ mode, the majority of energy is either in the shell or the liquid depending upon whether the excitation is structural or located in the liquid. The ratio of powers between the liquid and shell vibrational fields is given by

$$E_r(n=0) = \frac{P_{fb}}{P_{sb}} = \Omega(k_{ns}R)\frac{\rho_f}{\rho_s}\frac{F_f}{S_f}\frac{1}{[k_s^r R \mathrm{J}_n'(k_s^r R)]^2}, \tag{8}$$

where P_{fb} is the liquid contribution and P_{sb} the structural contribution to the energy flow due to the bending motion, F_f is the fluid factor and S_f is the shell factor [27].

In Fig. 6 is shown typical energy ratios for normal propagating modes in a metal pipe filled with water for the $n = 0$ mode, where s is the branch number of the dispersion curves for a water-filled shell. The $s = 1$ is the fluid branch and the $s = 2$ is the shell wave branch. At low frequencies ($\Omega < 1$) for the $n = 0$ mode, most of the energy is located in the pipe wall for the structural excitation. For excitation in the liquid, most of the energy remains in the liquid.

The first order mode, at frequencies far below the ring frequency, corresponds to a bending wave in a slender beam and the vibrational energy is nearly all in the pipe wall [27]. Pavić [29] has investigated the vibrational energy flow through straight pipes and has demonstrated that the liquid contribution to the energy flow due to the bending motion will be usually negligible in comparison with the structural contribution. The ratio between the two can be found from

$$E_r(n=1) = \frac{P_{fb}}{P_{sb}} = \frac{\Omega\eta}{8\sqrt{2+\eta}}, \tag{9}$$

where η is the non-dimensional constant: $\eta = (\rho_f/\rho_s)(R/h)$. For a copper pipe with $R = 0.011$ m and $h = 0.0009$ m, and for $\Omega \leqslant 0.044$, which corresponds to the frequency range 0–2.5 kHz, this ratio is $E_r(n=1) \leqslant 4.1 \times 10^{-3}$.

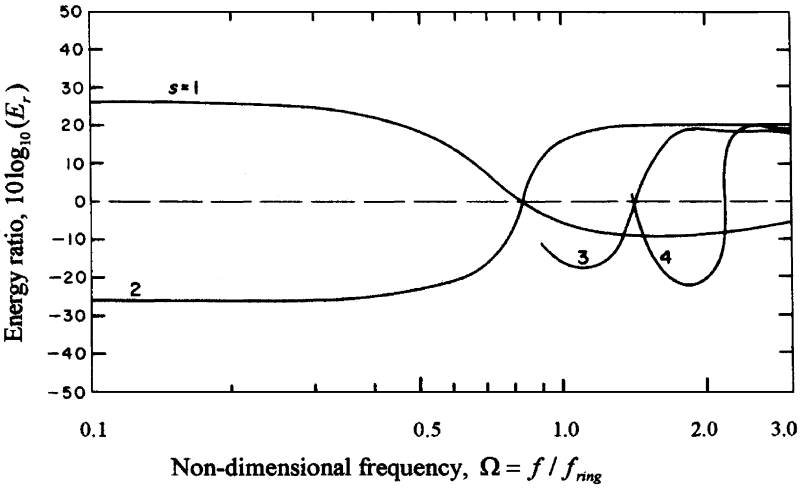

Fig. 6. Distribution of vibrational energy in a water-filled steel shell of thickness $h/R = 0.05$ for $n = 0$ (after Ref. [20]).

7. Energy flow through straight pipes

The propagation of vibroacoustic waves in liquid-filled cylindrical shells is further complicated due to the interchange of energy along the pipe not only between the different modes but also between the solid pipe and the liquid. However, from the above discussion it can be seen that at low non-dimensional frequencies, only those modes for $n = 0$ and 1 need be considered. The total energy flow in a liquid-filled cylindrical pipe for $n = 0$ and 1 modes is

$$P = P_T + P_L + P_{B1} + P_{B2} + P_F + P_{LF} + P_{B1F} + P_{B2F} + P_{FL} + P_{FB1} + P_{FB2}, \tag{10}$$

where P_T is the energy flow by the torsional wave in the pipe wall. P_L is by the longitudinal wave in the pipe wall. P_B is by the bending wave in the pipe wall; there are two bending terms because of two allowed polarizations. P_F is by the plane wave in the contained liquid. P_{LF}, P_{B1F} and P_{B2F} are the structural energy components in the pipe wall generated by the plane wave in the contained liquid. P_{FL}, P_{FB1} and P_{FB2} are the structural contributions to the energy flow in the liquid. P_{B1F} and P_{B2F}, the liquid contributions to the energy flow due to the bending motions, are very small, and can be neglected. For structure excitations, most of the energy is in the pipe wall, and P_{FL}, P_{FB1} and P_{FB2} can be neglected. For the case of excitation in the liquid, most of the energy is in the liquid and P_{LF}, P_{B1F} and P_{B2F} can be neglected. The total structure-borne energy flow P_s and total liquid-borne energy flow P_f can be estimated from

$$P_s = P_T + P_L + P_{B1} + P_{B2}, \tag{11}$$

$$P_f = P_F. \tag{12}$$

For the case where both structural and liquid excitations occur, Eq. (10) can be simplified to

$$P = P_T + P_L + P_{B1} + P_{B2} + P_F. \tag{13}$$

In a straight liquid-filled pipe with low turbulence, there will be little mode conversion. The energy flow components on the right side of Eq. (13) can be assumed independent and practically measurable.

8. Structure-borne power into semi-infinite pipes

Vibrating pumps will apply forces and moments to the connected pipes. The active power for each component of excitation is obtained from Eq. (1), as illustrated in Fig. 3. The source data include free velocity and mobility of the pump for six degrees of freedom; the receiver data are force and moment mobilities at the connecting point of the pipe. For the co-ordinate system that is shown in Fig. 3, a pump can apply the following excitation components to the connected pipe:

F_x excites a quasi-longitudinal wave in the x direction.
F_y excites a bending wave with displacement in the y direction.
F_z excites a second bending wave in the z direction.
M_x is the moment about the x-axis and excites a torsional wave about the cylindrical section.
$M_{y,z}$ are the moments about the y-, z-axis that induce polarized bending waves in the y, z directions.

Quasi-longitudinal, bending and torsional waves carry the most of the structure-borne energy in the low frequencies and will be investigated in detail. Although, consideration of the source descriptor has shown that the rotational components of the pump excitation can be neglected, they are considered further in order to confirm this simplifying assumption.

A pump with an activity in the axial direction of a connected semi-infinite pipe will generate a quasi-longitudinal wave with a power given by Eq. (1)

$$P_L = \frac{1}{2}\frac{(v_{sfx})^2}{\left|\tilde{Y}_{sL} + \tilde{Y}_{rL}\right|^2}\mathrm{Re}\{\tilde{Y}_{rL}\}, \tag{14}$$

where v_{sfx} is the pump free velocity in x direction, $\tilde{Y}_{sL}$ is point force mobility of the pump, and $\tilde{Y}_{rL}$ is point force mobility of the receiving structure, a semi-infinite pipe. v_{sfx} and $\tilde{Y}_{sL}$ were measured directly. $\tilde{Y}_{rL}$ is obtained from [31]

$$\tilde{Y}_{rL} = \frac{1}{\rho S c_{LII}}. \tag{15}$$

S is the area of the beam cross-section and c_{LII} is the velocity of the longitudinal wave. For a semi-infinite copper pipe with $R = 0.011$ m and $h = 0.0009$ m, the quasi-longitudinal power emission has been calculated by using Eqs. (14) and (15) and a typical result is shown in Fig. 7.

In addition, two polarized bending waves will be generated with powers given by

$$P_B = \frac{1}{2}\frac{(v_{sf})^2}{\left|\tilde{Y}_{sB} + \tilde{Y}_{rB}\right|^2}\mathrm{Re}\{\tilde{Y}_{rB}\}, \tag{16}$$

where v_{sf} is pump free velocity in the y or z direction, $\tilde{Y}_{sB}$ is the component point force mobility of the pump, and $\tilde{Y}_{rB}$ is the component point force mobility of the semi-infinite pipe. At low

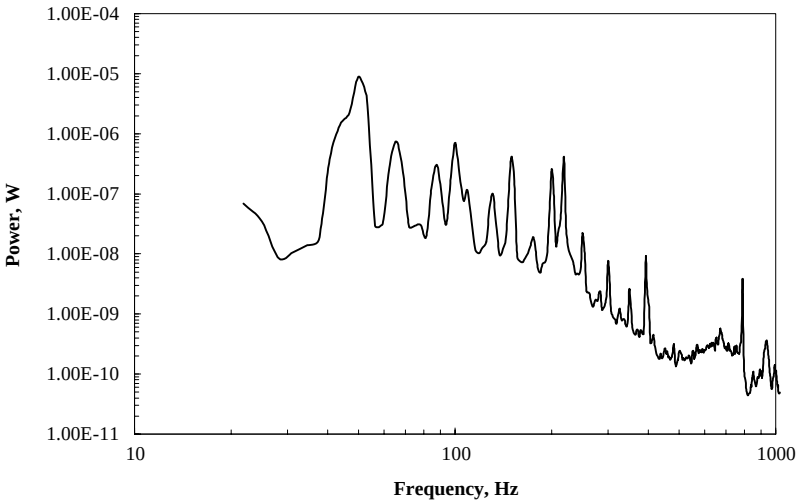

Fig. 7. Quasi-longitudinal power into a semi-infinite pipe.

frequencies (for $\Omega = \omega R/c_{LI} < 0.77h/R$) the mobility of a pipe is very nearly equal to that of a beam with radius of gyration $R/\sqrt{2}$, given by [31]

$$\tilde{Y}_{rB} = \frac{1}{\rho S c_B}\frac{2}{(1+\mathrm{j})} \approx \frac{1}{0.67\rho S\sqrt{c_{LI}hf}}\frac{1}{(1+\mathrm{j})}, \tag{17}$$

where $S = ((R/\sqrt{2})\sqrt{12})^2 = 6R^2$ is the area of the beam cross-section.

For a water-filled copper pipe with $R = 0.011m$ and $h = 0.0009m$, c_B is decreased 10% on average, compared with the in vacuo value. This did not significantly alter trends identified in analysis of the in vacuo case, which was used subsequently.

The rotational excitations about the y and z axes also induce two polarized bending waves with power

$$P_{B\omega} = \frac{1}{2}\frac{(v_{sf\omega})^2}{\left|\tilde{Y}_{s\omega} + \tilde{Y}_{r\omega}\right|^2}\mathrm{Re}\{\tilde{Y}_{r\omega}\}, \tag{18}$$

where $v_{sf\omega}$ is free angular velocity of the pump about the y and z direction, $\tilde{Y}_{s\omega}$ is the component point moment mobility of the pump, and $\tilde{Y}_{r\omega}$ is the component point moment mobility of the semi-infinite pipe, obtained from [31]

$$Y_{r\omega} = \frac{k_B^2}{\rho S\sqrt{\omega c_{LI}\dfrac{R}{\sqrt{2}}}}(1+\mathrm{j}). \tag{19}$$

For a copper pipe with $R = 0.011$ m and $h = 0.0009$ m, the bending powers induced through forces and moments have been calculated by using Eqs. (16)–(19). A force-induced bending power and a moment-induced power, in the same direction, are shown in Fig. 8. The moment-induced power is of the order of 30 dB less than that induced by the force and confirms the earlier decision

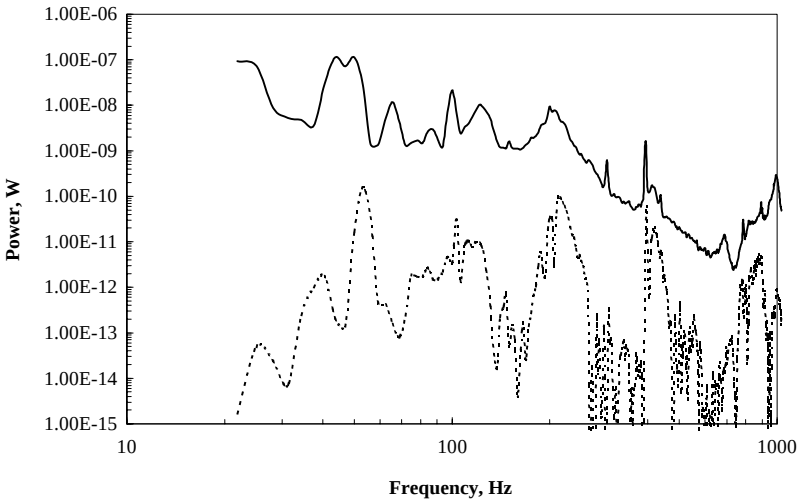

Fig. 8. Power into a semi-infinite pipe: ——, force induced bending power; - - - - -, moment-induced bending power.

to neglect it, based on measured source descriptors. Similarly, the power induced by the torsional component (not shown) was small and could be neglected.

9. Predicted and measured bending power

The structure-borne sound power was predicted according to Eq. (16). For the purpose of comparison, bending power was measured using a structural intensity method. The bending waves are the easiest to damp. A sandbox was used to absorb the bending waves on a copper pipe so that the pipe could be treated as a semi-infinite system. Tests were conducted on a 6 m copper pipe with $R = 0.011$ m and $h = 0.0009$ m. The pipe was partly buried in the sandbox from 2.5 m onwards (Fig. 9). To confirm that the sandbox efficiently damped the bending waves and that the structure-borne power was little influenced by liquid-loading, the bending mobilities of the pipe were measured for the pipe when empty and when filled with water, using a calibrated hammer method [37,38]. In Fig. 10 are shown measured bending mobilities for the filled and empty pipes and predicted results. There is low frequency fluctuation about the theoretical line, indicating that resonances are not fully damped. The agreement is better between 200 and 1500 Hz. The fluctuation in value is greater for the water-filled pipe than that for empty pipe. This is due to the effect of reflected liquid waves which are generated by the vibration of the pipe wall.

The change in mobility due to liquid loading is of the order of 0.5 dB and can be neglected. In the test rig, shown in Fig. 9, the pump was connected inline with the pipe and the inlet of the pump and far end of the 'semi-infinite' copper pipe were connected by a flexible pipe to allow circulation. The matched accelerometer pair was located at a distance greater than one half-wavelength (for 20 Hz, the wavelength is 3 m) from the pump to avoid nearfield effects.

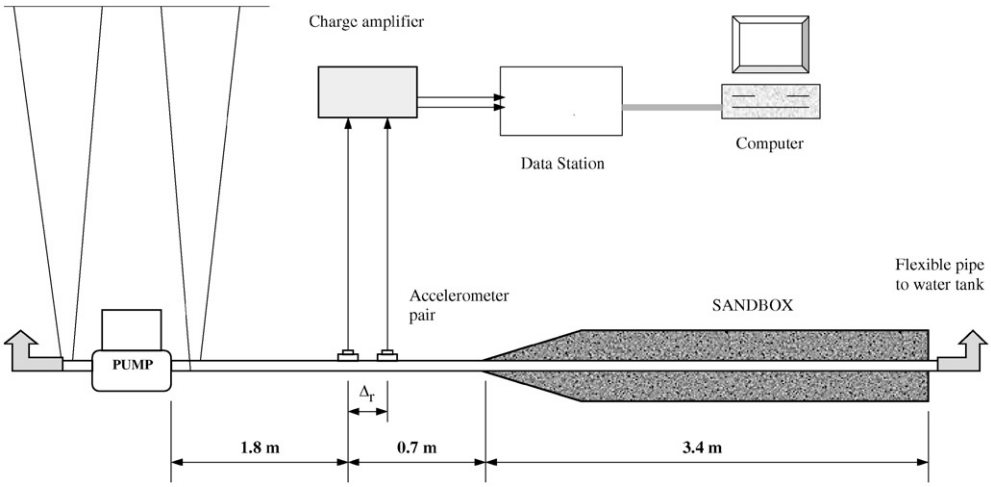

Fig. 9. Test rig for bending power measurement on a pipe.

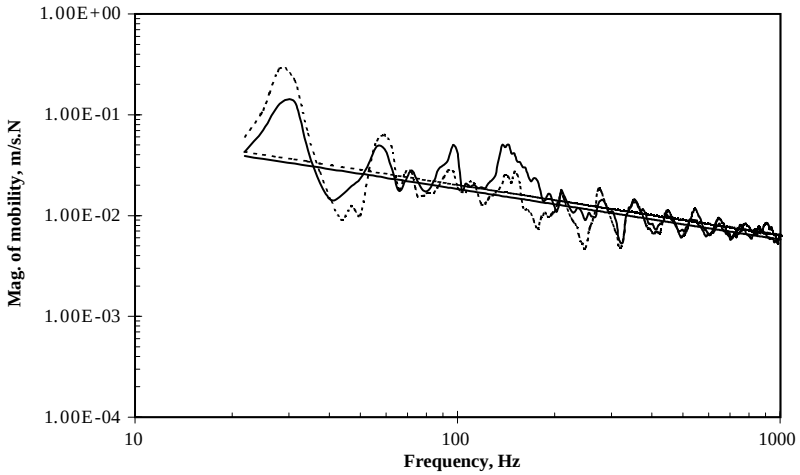

Fig. 10. Mobility of semi-infinite copper pipe: ——, without water, predicted and measured; - - - - -, filled with water, measured and predicted.

The time-averaged bending power, in the frequency domain, can be expressed as [39]

$$P_B = \frac{2(Bm')^{1/2}}{\Delta} \int_0^\infty \frac{\mathrm{Im}[G(a_1, a_2, f)]}{\omega^2} \mathrm{d}f, \tag{20}$$

where B is the bending stiffness, m' is the mass per length, Δ is the distance between the two accelerometers and Im[G] is the imaginary part of the cross spectral density between the acceleration a_1 and a_2.

The measured and predicted bending powers are shown in Fig. 11. In general, results are within 5 dB for most of frequencies above 100 Hz. Below 100 Hz, the difference can be as much as 20 dB.

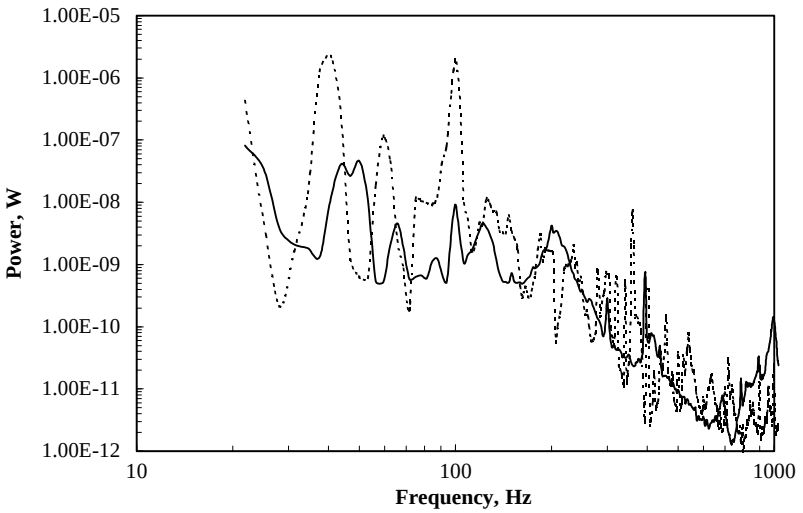

Fig. 11. Bending power into a semi-infinite pipe: - - - - -, measured; ——, predicted.

There are more peaks on the measured power curve, due to imperfections in the pipe system. Also there are shifts in the pump rotation frequency, its harmonics and pump impeller 'cut water' frequency, between 350 and 400 Hz. This was because of small changes in operating conditions between the rig for the free velocity measurements and the present rig, despite efforts to control flow speed (typically 1.2 m/s), pressure and temperature. For the predicted power, the free velocity was measured when the pump was connected to the flexible pipes, and for the power measurement the pump was connected to a semi-infinite copper pipe, on its outlet side. The results show that the mobility method can be used to calculate the bending power flow from a pump into a semi-infinite pipe. The same therefore was assumed to apply for quasi-longitudinal waves.

10. Liquid-borne power into semi-infinite pipes

The liquid-borne sound, or pressure ripple, generated by pumps is transmitted via the liquid to remote parts of the circuit where it can cause problems such as airborne noise, vibration and instability. In domestic installations, liquid-borne and structure-borne transmissions occur simultaneously and both may contribute significantly to the radiated sound in the far field, so that it is important that both can be included on a power basis in a source characterization [1].

For the liquid-borne emission, direct measurement is a practical possibility because a semi-infinite condition is relatively easy to produce in the laboratory. A flexible pipe can be used as a non-reflecting receiver. The attenuation produced by a flexible rubber pipe of internal diameter 20 mm, wall thickness 3 mm and of different lengths was measured, using an impulse method. The measurement set-up is shown in Fig. 12. A small shaker was used to excite a pressure ripple in the flexible pipe through a small cylinder. Two pressure transducers were located on a flexible pipe of length of 20 m to measure the attenuation produced by the flexible pipe of different lengths Δl. The two measured pressures, over a distance of 5 m, are shown in Fig. 13. The level difference is of

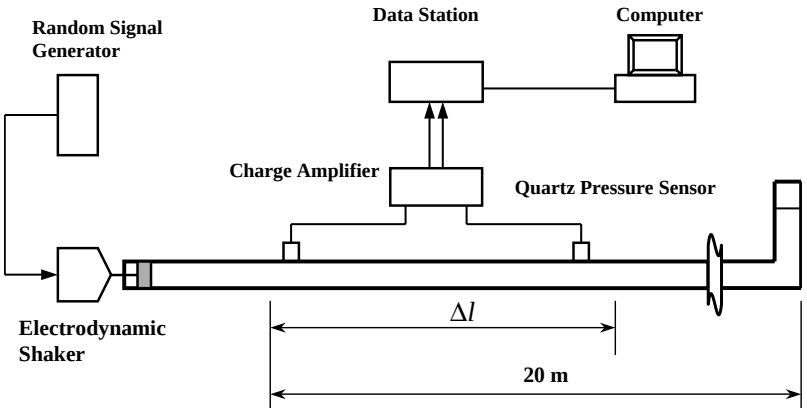

Fig. 12. Set-up for the measurement of flexible pipe attenuation.

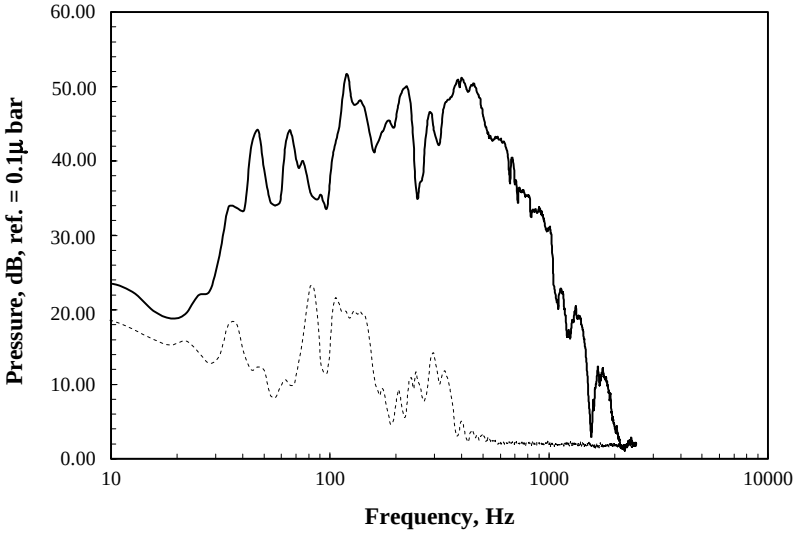

Fig. 13. Measured pressure in a flexible pipe of internal diameter 20 mm: ——, at first transducer near excitation end; - - - - -, 5 m from first transducer.

the order of 20 dB for frequencies up to 100 Hz, and 30 dB for frequencies between 100 and 500 Hz. Above 500 Hz, the pressure ripple is attenuated to the background noise level.

Liquid-borne sound emission from the pump can be measured by using an intensity method [40–43] analogous to Eq. (20) for bending wave intensity. The sound intensity in a frequency range $[f_1, f_2]$ is

$$I_{\Delta f} = -\frac{1}{2\pi\rho\Delta r}\int_{f_1}^{f_2}\frac{\mathrm{Im}[G_{AB}(p_A, p_B, f)]}{f}\,\mathrm{d}f, \tag{21}$$

where $\mathrm{Im}[G_{AB}]$ is the imaginary part of the cross spectral density between the pressure p_A and p_B, and Δr is the distance between the two pressure transducers. Errors increase as Δr decreases. For an error of ± 0.5 dB, $k\Delta r < 0.8$, or $f\Delta r < 189$ [41]. In this study, Δr was set at 30 mm.

The measured liquid-borne sound power is shown in Fig. 14. The predicted quasi-longitudinal power and that of one of the polarized bending waves are included for comparison. Below 200 Hz, the pump is predominantly a liquid-borne source. Above 200 Hz, it is a structure-borne source.

All of the components of structure-borne power emission from a pump into a semi-infinite pipe were obtained and are shown in Fig. 15. The moment-induced torsional emission and

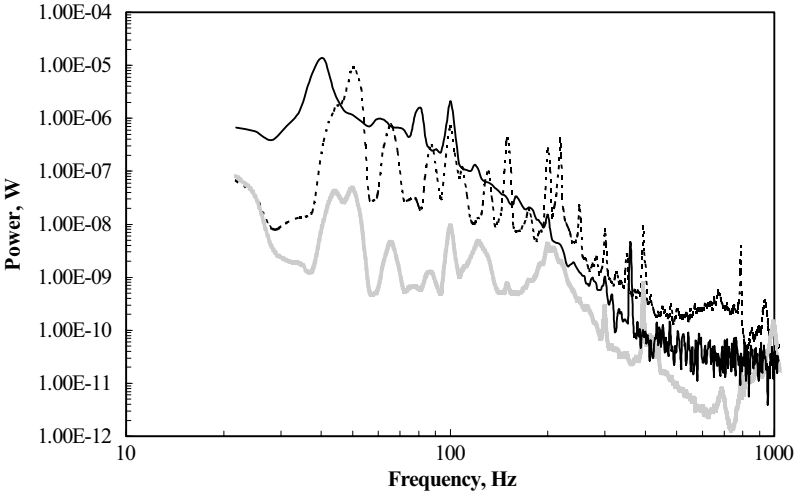

Fig. 14. Power into a semi-infinite pipe:——, measured fluid-borne power; - - - - -, predicted quasi-longitudinal power; ——, predicted bending power.

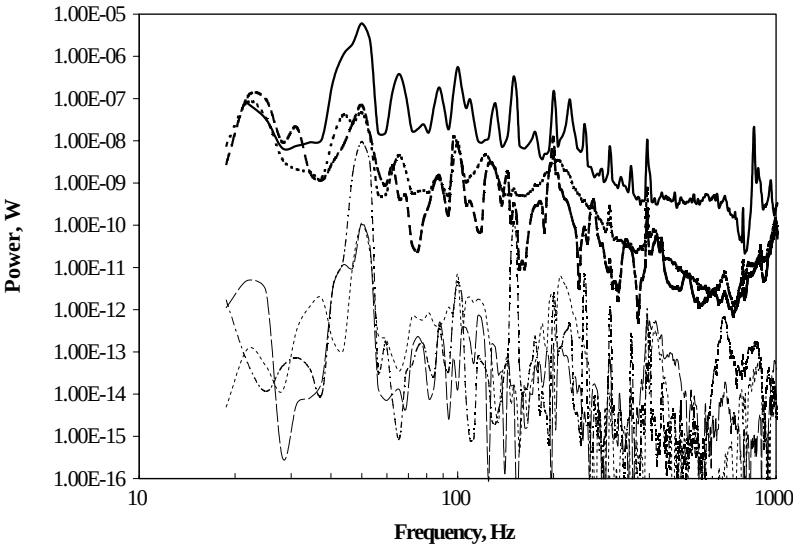

Fig. 15. Structure-borne power into a semi-infinite pipe: ——, force induced quasi-longitudinal emission; · · · · ·, force induced bending; - - - - -, force induced second bending; - - - - -, moment induced torsional; –·–·–·–·, moment induced bending; ——, moment induced second bending.

two moment-induced bending emission components are much lower than force-induced quasi-longitudinal and two polarized bending emission components, and can be neglected. The longitudinal wave is the dominant component of the structure-borne power and is at a similar level as the liquid-borne power. Though the bending power is lower than the longitudinal and liquid-borne power it cannot be neglected at this stage since the acoustic radiation in the central heating system ultimately results from the bending vibration. In the central heating system, an axial component or a bending wave excited by the pump will partially convert to other modes of vibration at pipe junctions before energizing the radiator.

11. Concluding remarks

A method has been proposed to obtain the acoustic power from central heating circulation pumps into semi-infinite pipe systems in order to characterize the pumps as structure-borne sound sources.

At low non-dimensional frequencies and for straight pipes the total power can be described in terms of the torsional, longitudinal, polarized bending and the plane pressure waves. The input structure-borne power will remain as structure-borne propagation. The input liquid-borne power will remain as liquid-borne propagation.

For the structure-borne source, the emission can be calculated from the measured free velocity and mobility of the pump for each component of vibration and from receiver mobilities of idealized pipe systems. For the pumps examined, the three moment-induced power components are much lower than force-induced power components and therefore can be neglected. The total structure-borne emission can be estimated from the quasi-longitudinal and two polarized bending powers.

The pumps investigated are predominately liquid borne sources below 200 Hz and structure-borne sources above 200 Hz.

Acknowledgements

The authors gratefully acknowledge the financial support of this study by the Engineering and Physical Sciences Research Council of the UK.

References

[1] N. Qi, A.T. Moorhouse, B.M. Gibbs, Investigation of appropriate measurements to characterise small domestic central pumps as sources of structure-borne sound, Proceedings of Euronoise 98 (1) (1998) 395–400.
[2] B.M. Gibbs, N. Qi, Fluid-borne and structure-borne sound emission from small circulation pumps, Proceedings of the Seventh International Congress on Sound and Vibration, Garmisch-Partenkirchen, 2000, pp. 1597–1604.
[3] ISO 3740–3747, Acoustics—Determination of sound power levels of noise sources.
[4] E.J.M. Nijman, B.A.T. Petersson, Airborne sound characterisation of automotive engines: the acoustical interface impedance concept, Proceedings of the 17th International Congress on Acoustics, Rome, 6C.12.02, 2001.
[5] ISO 10767-1, Hydraulic liquid power—determination of pressure ripple levels generated in systems and components, 1996.

[6] ISO/CD 1690-2, Hydraulic liquid power—test code for the determination of sound power levels of pumps using sound intensity techniques, 1999.
[7] ISO 3822, Acoustics—laboratory tests on noise emission from appliances and equipment used in water supply installations, 1983.
[8] B.M. Gibbs, B.A.T. Petersson, Rating of machines as structure-borne sound sources, Proceedings of the Institute of Acoustics 17 (1995) 139–146.
[9] C.A.F. de Jong, Analysis of Pulsations and Vibrations in Liquid-filled Pipe Systems, Ph.D. Thesis, TNO Institute of Applied Physics, Delft, Netherlands, 1994.
[10] B.A.T. Petersson, Preliminaries for pure transfer mobilities: beam- and frame-like structures, TNO-Report, TPD-HAG-RPT-93-0157, Delft, Netherlands, 1993.
[11] B.M. Gibbs, Structure-borne sound sources in buildings, Building Acoustics 1 (4) (1994) 313–329.
[12] J.M. Mondot, B.A.T. Petersson, Characterization of structure-borne sound sources: the source descriptor and the coupling function, Journal of Sound and Vibration 114 (3) (1987) 507–518.
[13] B.A.T. Petersson, B.M. Gibbs, Use of the source descriptor concept in studies of multi-point and multi-directional vibrational sources, Journal of Sound and Vibration 168 (1) (1992) 157–176.
[14] A.T. Moorhouse, and B.M. Gibbs, Measurement of the characteristic power of structure-borne sound sources, Proceedings of the Sixth International Congress on Sound and Vibration, Lyngby, 1999, pp. 2161–2168.
[15] A.T. Moorhouse, B.M. Gibbs, Calculation of the mean and maximum mobility for concrete floors, Applied Acoustics 45 (1995) 227–245.
[16] A.T. Moorhouse, B.M. Gibbs, Prediction of the structure-borne noise emission of machines: development of a methodology, Journal of Sound and Vibration 167 (2) (1993) 223–237.
[17] ISO 9611, Characterisation of sources of structure-borne sound with respect to sound radiation from connected structures—measurements of velocity at the contact points of machinery when resiliently mounted, 1996.
[18] N. Qi, A.T. Moorhouse, B.M. Gibbs, Investigation of appropriate measurements to characterise small domestic central pumps as sources of structure-borne sound, Proceedings of Euronoise 98 (1) (1998) 395–400.
[19] A.T. Moorhouse, B.M. Gibbs, Measurement of the characteristic power for structure-borne sound sources, Proceedings of the Sixth International Congress on Sound and Vibration, Lyngby, 1999, pp. 2161–2168.
[20] BS 3015, Glossary of terms relating to mechanical vibration and shock, 1976.
[21] ISO 7626 1/2, Vibration and shock—experimental determination of mechanical mobility, 1986.
[22] B.A.T. Petersson, On the use of giant magnetostrictive devices for moment excitation, Journal of Sound and Vibration 116 (1987) 191–194.
[23] B.M. Gibbs, B.A.T. Petersson, Moment excitation and mobility measurement in studies of structure-borne emission, Acoustics Bulletin of IOA, May/June 1993.
[24] B.A.T. Petersson, B.M. Gibbs, Towards a structure-borne sound source characterization, Applied Acoustics 61 (2000) 325–343.
[25] B.M. Gibbs, A.T. Moorhouse, Case studies of machine bases as structure-borne sound sources in buildings, International Journal of Acoustics and Vibration 4 (3) (1999) 125–133.
[26] B.A.T. Petersson, Moment excitation and structural acoustic power transmission between machinery and foundations, TNO Industrial Research Report TPD-SA_RPT-90–149, 1990.
[27] C.R. Fuller, F.J. Fahy, Characteristics of wave propagation and energy distribution in cylindrical elastic shells filled with liquid, Journal of Sound and Vibration 81 (4) (1982) 501–518.
[28] G. Pavić, Vibrational energy flow in elastic circular cylindrical shells, Journal of Sound and Vibration 142 (2) (1990) 293–310.
[29] G. Pavić, Vibroacoustical energy flow through straight pipes, Journal of Sound and Vibration 154 (3) (1992) 411–429.
[30] W. Soedel, Vibrations of Shells and Plates, Marcel Dekker, New York, 1981.
[31] L. Cremer, M. Heckl, E.E. Ungar, Structure-borne Sound, Springer, New York, 1988.
[32] A.W. Leissa, Vibration of Shells, Acoustical Society of America, 1993.
[33] R.J. Pinnington, A.R. Bruce, Externally applied sensor for axisymmetric waves in a fluid filled pipe, Journal of Sound and Vibration 173 (4) (1994) 503–516.

[34] C.R. Fuller, The effects of wall discontinuities on the propagation of flexural waves in cylindrical shells, Journal of Sound and Vibration 75 (1981) 207–228.
[35] P.H. White, R.J. Sawley, Energy transmission in piping systems and its relation to noise control, Transactions of the ASME, Journal of Engineering for Industry (May 1972) 746–751.
[36] P.G. Bentley, D. Firth, Calculation of basic resonances for acoustic vibration in fast reactors, Computers and Structures 6 (1976) 187–192.
[37] R.J.M. Craik, Damping of building structures, Applied Acoustics 14 (1981) 347–359.
[38] A.T. Moorhouse, Structure-borne Emission of Installed Machinery in Buildings, Ph.D. Thesis, The University of Liverpool, 1989.
[39] J.W. Verheij, Cross spectral density methods for measuring structure-borne power flow on beams and pipes, Journal of Sound and Vibration 70 (1980) 133–138.
[40] F.J. Fahy, Measurement of the acoustic intensity using the cross-spectral density of two microphone signals, Journal of the Acoustical Society of America 62 (1977) 1057–1059.
[41] F.J. Fahy, Sound Intensity, Elsevier Applied Science, Oxford, 1989.
[42] J.W. Verheij, Cross spectral density methods for measuring structure-borne power flow on beams and pipes, Journal of Sound and Vibration 70 (1980) 133–138.
[43] J.Y. Chung, Cross spectral method of measuring acoustic intensity without error caused by instrument phase mismatch, Journal of the Acoustical Society of America 64 (1978) 1613–1616.